Computer Applications in Electrical Engineering
Vol. 13 *2015*

Model of magnetic gun with respecting eddy currents

Karel Leubner, Ivo Doležel, Radim Laga
Czech Technical University
166 27 Praha 6, Technická 2, Czech Republic, e-mail: dolezel@fel.cvut.czz

A sophisticated mathematical model of the magnetic gun is presented and solved numerically. The model consists of three strongly non-linear and non-stationary differential equations describing the time-dependent distribution of magnetic field in the device, current in the field circuit and movement of the projectile. The numerical solution is carried out in the application Agros2D based on a fully adaptive higher-order finite element method. The results are processed in Wolfram Mathematica. The methodology is illustrated with an example and selected results are compared with experiment.

KEYWORDS: magnetic gun, magnetic field, numerical solution, higher-order finite element method, coupled problem

1. Introduction

Magnetic guns are devices based on the effect of magnetic forces on ferromagnetic projectiles. Although their principle has been known for more than 150 years, the history of their research began only in the times of the World War I [1]. But as the electromagnetic aspects of the device and movement of the projectile were investigated separately, the results could be considered just approximate.

The structure of a magnetic launcher is relatively simple. The main parts of the device (see Fig. 1) are a field coil, a barrel made of plastic or a suitable metal (in this case it must contain a longitudinal gap to suppress generation of induced currents) and a ferromagnetic projectile.

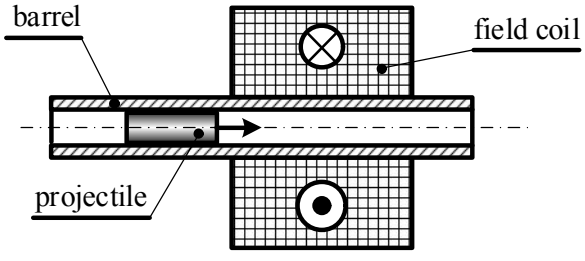

Fig. 1. Main parts of the launcher

The field coil is fed from a charged capacitor battery (which is better than a classic battery because the internal resistance of the battery is higher and energy from it cannot be transferred as fast as necessary). The corresponding external circuit is depicted in Fig. 2.

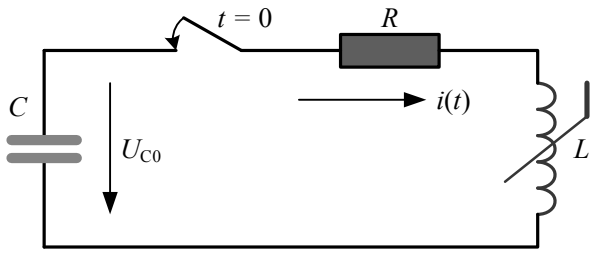

Fig. 2. Arrangement of the external circuit

At the moment of switching the circuit (time $t = 0$), it starts carrying time-variable current $i(t)$ of pulse character. This current generates in the field coil corresponding magnetic field that attracts the ferromagnetic projectile into its center. But as soon as the projectile reaches approximately its center, the circuit must be switched off and since then it continues moving only due to inertia forces (in case that the coil would continue carrying the current, the projectile would start to be decelerated).

2. Mathematical model

The mathematical model consists of three strongly non-linear differential equations. The first of them is ordinary and describes the time evolution of the field current $i(t)$. The governing equation reads

$$Ri + \frac{\mathrm{d}}{\mathrm{d}t}(Li) + \frac{1}{C}\int_0^t i \,\mathrm{d}\tau = U_{C0}, \tag{1}$$

and the initial conditions is

$$i(0) = 0, \quad \frac{\mathrm{d}i(0)}{\mathrm{d}t} = \frac{U_{C0}}{L_0}. \tag{2}$$

Here, symbol R stands for the overall resistance of the circuit, L is the inductance of the field coil (L_0 being its initial value), C represents the capacitance of the battery, and U_{C0} denotes its initial voltage. The inductance L is a non-linear function of the position and velocity of the projectile and also of the field current.

Motion of the projectile obeys another ordinary differential equation in the form

$$m\frac{\mathrm{d}\boldsymbol{v}}{\mathrm{d}t} = \boldsymbol{F}_{\mathrm{em}} - \boldsymbol{F}_{\mathrm{dr}}, \quad \boldsymbol{v} = \frac{\mathrm{d}\boldsymbol{s}}{\mathrm{d}t}, \tag{3}$$

with the initial conditions

$$\boldsymbol{v}(0) = 0, \qquad \boldsymbol{s}(0) = \boldsymbol{s}_0 . \tag{4}$$

Here, m denotes the mass of the projectile, $\boldsymbol{v}$ represents its velocity, $\boldsymbol{F}_{\mathrm{m}}$ is the magnetic force acting on it and $\boldsymbol{F}_{\mathrm{d}}$ stands for the sum of the drag forces (that are given by the friction in the barrel and aerodynamic force). The magnetic force $\boldsymbol{F}_{\mathrm{m}}$ is also a strongly nonlinear function of the position and velocity of the projectile and of the field current.

Both values of inductance L and magnetic force $\boldsymbol{F}_{\mathrm{m}}$ must be determined from the actual distribution of magnetic field. For example, the distribution of vector magnetic potential in it is given by a non-linear partial differential equation in the form [2]

$$\operatorname{curl}\left(\mu^{-1}\operatorname{curl}\boldsymbol{A}\right) + \gamma\left(\frac{\partial \boldsymbol{A}}{\partial t} - \boldsymbol{v}\times\operatorname{curl}\boldsymbol{A}\right) = \boldsymbol{J}_{\mathrm{ext}}, \tag{5}$$

where μ denotes the magnetic permeability, γ stands for the electrical conductivity, and $\boldsymbol{J}_{\mathrm{ext}}$ is the field current density in the field coil, for which there holds

$$\int_S \boldsymbol{J}_{\mathrm{ext}}(t)\cdot\mathrm{d}\boldsymbol{S} = i(t), \tag{6}$$

where S is the cross section of one turn of the field coil.

The boundary condition along a sufficiently distant boundary is of the Dirichlet type.

The term $-\gamma\left(\partial\boldsymbol{A}/\partial t - \boldsymbol{v}\times\operatorname{curl}\boldsymbol{A}\right)$ represents the total density of currents induced in the system. The first term $-\gamma\cdot\partial\boldsymbol{A}/\partial t$ represents eddy current densities due to the time variations of magnetic field while the second term $\gamma\boldsymbol{v}\times\operatorname{curl}\boldsymbol{A}$ denotes eddy current densities due to the movement. Their force effects act again the magnetic force $\boldsymbol{F}_{\mathrm{m}}$ and generally lead to a deceleration of the projectile.

The inductance L (as one of the input quantities to (1)) can be determined using the formula

$$L = \frac{2W_{\mathrm{m}}}{i^2}, \tag{7}$$

where W_{m} is the energy of magnetic field of the system that may be calculated using the formula

$$W_{\mathrm{m}} = \frac{1}{2}\int_V \boldsymbol{J}\cdot\boldsymbol{A}\,\mathrm{d}V . \tag{8}$$

Here, $\boldsymbol{J}$ denotes the total current density at a point and the integration is carried out over the volume V in which $|\boldsymbol{J}| > 0$.

The total magnetic force $\boldsymbol{F}_{\mathrm{m}}$ (including the effects of the induced currents) follows from the formula [3]

$$\boldsymbol{F}_{\mathrm{m}} = \oiint_S \boldsymbol{T}_{\mathrm{m}} \mathrm{d}\boldsymbol{S}, \tag{9}$$

where $\boldsymbol{T}_{\mathrm{m}}$ is the magnetic Maxwell stress tensor. This can be expressed in the form

$$\boldsymbol{T}_{\mathrm{m}} = \boldsymbol{H} \otimes \boldsymbol{B} - \frac{1}{2}(\boldsymbol{H} \cdot \boldsymbol{B})\boldsymbol{I}, \tag{10}$$

where $\boldsymbol{H}$ and $\boldsymbol{B}$ are the vectors of magnetic field strength and magnetic flux density, respectively ($\boldsymbol{B} = \operatorname{curl} \boldsymbol{A}$, $\boldsymbol{B} = \mu \boldsymbol{H}$, μ being scalar quantity), $\boldsymbol{I}$ stands for the unit matrix, and symbol $\otimes$ represents the dyadic product. The integration in (9) is performed over the closed boundary of the projectile.

3. Numerical solution of the model

The three basic equations (1), (3) and (5) should be, due to non-linear properties, solved simultaneously. A number of codes allow combining the field equation (5) and field current equation (1), but problems are still with the inclusion of the equation (3).

The task was numerically solved by several authors [4–7], always under certain simplifying assumptions. The influence of the induced currents due to movement of the projectile was mostly neglected. In other cases, linearization techniques were applied to cope with strong nonlinearities, etc. The paper presents another technique based on the approximation of the first pulse of the field current by a sinusoidal function.

This approach is based on a small difference between the inductance L of the field coil with and without the projectile, which reaches in common cases not more than about 5 %. In such a case, (1) can be solved with a medium value L_{m} of the inductance L instead of its variable value. This provides a damped oscillatory solution, whose first pulse can be, with a very good accuracy, considered sinusoidal. With a sinusoidal field current, the field equation (5) can be transformed (again with an acceptable error) into the phasor form

$$\operatorname{curl}(\operatorname{curl} \underline{\boldsymbol{A}}) + \mu\gamma\left(\mathrm{j} \cdot \omega \underline{\boldsymbol{A}} - \boldsymbol{v} \times \operatorname{curl} \underline{\boldsymbol{A}}\right) = \mu \underline{\boldsymbol{J}}_{\mathrm{ext}}, \tag{11}$$

where ω denotes the angular velocity corresponding to the period of the function approximating the real time evolution of $i(t)$. But the magnetic permeability of the projectile is not constant; it is considered constant just in every cell of the discretization mesh, where it is assigned to the corresponding

value of magnetic flux density $|\boldsymbol{B}|$, according to the saturation curve of the material used.

The next step is repeated calculation of (11) with to obtain the nomograms of L and $\boldsymbol{F}_{\mathrm{m}}$ as functions of current i and position $\boldsymbol{s}$ of the projectile, for various values of its velocity $\boldsymbol{v}$. The nomograms are then used for interpolative and extrapolative determination of the values of L and $\boldsymbol{F}_{\mathrm{m}}$ for the real values of the current and position and velocity of the projectile.

The task was solved numerically by the combination of our own application Agros2D [8] and commercial software Wolfram Mathematica. The code Agros2D (open source) is based on a fully adaptive higher-order finite element method and is intended for numerical solution of 2D nonlinear and nonstationary multiphysics problems described by a set of partial differential equations. It is characterized by a number of quite unique features such as finite elements up to the 10^{th} order, efficient multi-mesh technology, dynamically changed meshes, hanging nodes of any level, combination of various elements including curvilinear elements (for approximation of curvilinear boundaries and interfaces) etc. The evaluation of the results and some auxiliary computations (for example, numerical integration of (1) and (3)) were carried out in Wolfram Mathematica using a lot of own procedures and scripts.

The algorithms of solution must cope with several serious problem. The principal one is connected with the computations of parts of nomograms of L and $\boldsymbol{F}_{\mathrm{m}}$ for high values of the field current i, which is accompanied with a strong or total oversaturation of the projectile. But this oversaturation may be evaluated only approximately, because the magnetization curve of material in the domain of high values of $|\boldsymbol{B}|$ can only be estimated. This leads to non-estimable errors of results, and, moreover, the related iterative processes are mostly accompanied by various undesirable phenomena such as oscillations, and generally, a very poor convergence rate, which means a long time of computations. This problem was solved by construction of a special function (dependent on parameters i and $\boldsymbol{s}$) that shows which parts of the projectile that may be replaced by air.

4. Illustrative example

The input data for the model were taken from the physical model of a magnetic gun completely built and tested by the third author. The device is shown in Fig. 3. It is a three-stage launcher, but the computations and measurements were carried out only on the first stage.

The principal dimensions of the coil of the first stage, leading barrel and projectile are depicted in Fig. 4. Their values are: $D_1 = 36$ mm, $d_1 = 8$ mm,

$L_1 = 50$ mm, $D_2 = 6.75$ mm, $L_2 = 52$ mm. The projectile in the barrel moves only in the x-direction and its initial position $x_0 = -38$ mm.

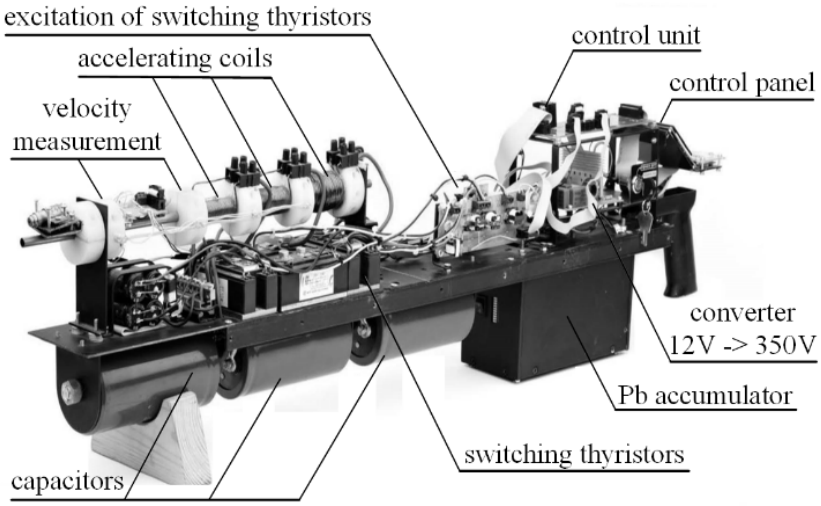

Fig. 3. Three-stage magnetic gun

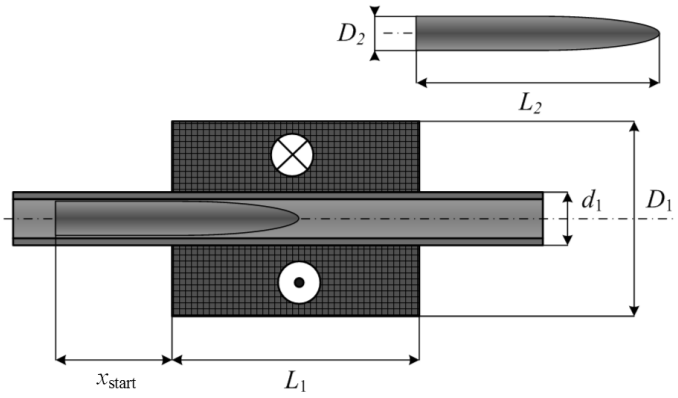

Fig. 4. Principal dimensions of the system

The voltage U_{C0} of the capacitor battery is 350 V. The parameters of the electric circuit were found for frequency 156 Hz, because the shape of the sinusoidal current corresponds to the shape of real current in the series RLC electric circuit. For the above frequency, the capacitance $C = 7.11$ mF, the total resistance of the circuit $R = 0.145$ Ω and inductance of the coil $L = 0.220$ mH. The coil contains 203 turns wound in 7 layers, each having 29 turns. The barrel is made of brass with a longitudinal gap. The projectile is made of ferromagnetic

material Vacoflux 48 (produced by German company Vacuumschmelze GmbH & Co). Its electric conductivity is 2.5 MS/m and mass density is 8120 kg m^{-3}. Its saturation curve is depicted in Fig. 5. The time step for the integration $\Delta t = 10^{-6}$ s.

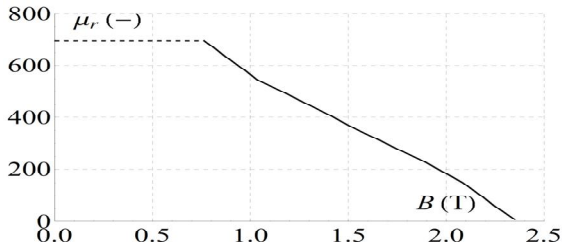

Fig. 5. Saturation curve of material Vacoflux 48

Figure 6 shows, for illustration, two nomograms $L(i,s)$ for velocity $v_x = 0$. The transparent one holds for the case without oversaturation, while the low one is the corrected nomogram that takes it into account (which is used for the computations).

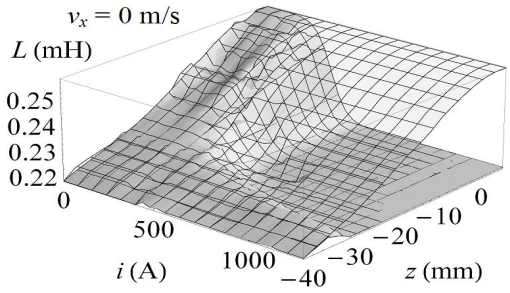

Fig. 6. Nomogram of inductance for $v_x = 0$

Important from the viewpoint of accuracy is the time evolution of current i in the field coil. This current was measured and also modelled using (1). The results are presented in Fig. 7. The measured line 1 shows the time evolution of the field current to the moment of its switching off (when the projectile reached the middle of the coil), i.e. about 2.9 ms. The line 2 shows the calculated evolution for circuit parameters measured at the industrial frequency. Finally, the line 3 shows the calculated time evolution for circuit parameters measured for frequency 156 Hz. Obviously, the accordance curves 1 and 3 is extremely good.

The time evolution of motion of the projectile was calculated using (2), where the drag force is represented by the aerodynamic resistance. Its value is given by the formula

$$F_{\mathrm{d},x} = \frac{1}{2} C \rho S v^2 \tag{11}$$

where ρ is the density of air, S is the area of the cross section of the projectile, and C is a constant. In our case $C = 0.4$.

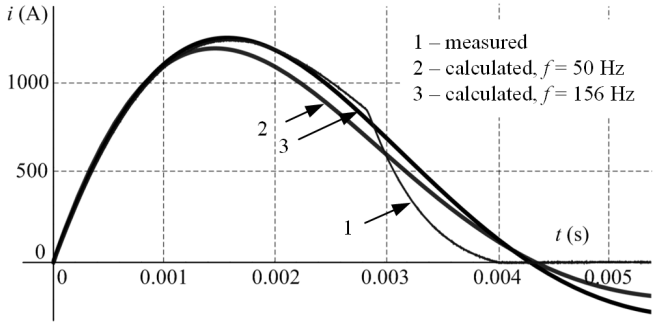

Fig. 7. Time evolution of the field current: 1 – measured, 2, 3 - calculated

Figure 7 depicts the time evolution of the position of the rear face of the projectile and Fig. 11 shows the time evolution of its velocity. The red lines are the dependences without respecting eddy currents in the projectile, the blue ones represent them. The differences are, however, very small. The eddy currents decelerate the velocity of the motion, but only very slightly.

Figure 8, left part, depicts the time evolution of the velocity of the projectile and right part shows the time evolution of its position. The computation were carried out with both respecting and not respecting the induced currents. The differences are, however, very small. For relatively low time changes of the field current and velocity their influence is still almost negligible.

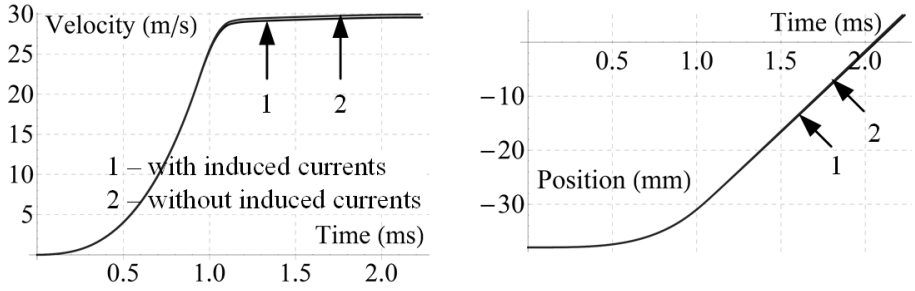

Fig. 8. Time evolution of velocity and trajectory of the projectile

The measured average muzzle velocity (determined from five measurements) on the device was 28.9 m/s. The difference from the calculated values is about 1 m/s (over 3 %), which can be considered excellent.

5. Conclusion

The model proved to provide realistic results whose agreement with the measured data is very good. Next work in the field will be focused on modelling all three stages of the electromagnetic gun.

Acknowledgment

This work was supported by the European Regional Development Fund and Ministry of Education, Youth and Sports of the Czech Republic (project No. CZ.1.05/2.1.00/03.0094: Regional Innovation Center for Electrical Engineering - RICE), by the project P102/11/0498 (Grant Agency of the Czech Republic) and project SGS-2012-039.

References

[1] di Gaeta, A., Glielmo, L., Giglio, V., Police, G., Modeling of an Electromechanical Engine Valve Based on a Hybrid Analytical-FEM Approach, IEEE/ASME Trans. Mechatr. 13 (2008), No. 6, pp. 625–637.

[2] Sun, Z., Kuo, T.-W., Transient Control of Electro-Hydraulic Fully Flexible Engine Valve Actuation System, IEEE Trans. Control Systems Technology 18 (2010), No. 3, pp. 613–621.

[3] Angadi, S. V., Jackson, R. L., Choe, S. Y., Flowers, G., T., Suhling, J. C., Chang, Y. K., Ham, J. K., Reliability and Life Study of Hydraulic Solenoid Valve. Part I - A Multi-physics Finite Element Model, Eng. Fail. Anal. 16 (2009), No. 3, pp. 874–887.

[4] Clark, R. E., Jewell, G., Forrest, S., Rens, J., Maerky, C., Design Features for Enhancing the Performance of Electromagnetic valve Actuation Systems, IEEE Trans. Magn. 41 (2005), No. 3, pp. 1163–1168.

[5] Liu, J. J., Yang, Y. P., Xu, J. H., Electromechanical Valve Actuation with Hybrid MMF for Camless Engine, proc. 17th World Congr. Int. Federation on Automatic Control, Seoul, Korea, July 6–11, 2008.

[6] Kim, J. H., Chang, J. H., A new Electromagnetic Linear Actuator for Quick Latching, IEEE Trans. Magn. 43 (2007), No. 4, pp. 1849–1852.

[7] Henrotte, F., Felden, M., Vander, G. M., Hameyer, K., The Eggshell Approach for the Computation of Electromagnetic Forces in 2D and 3D, COMPEL 23 (2004), No. 4, pp. 996–1005.

[8] Karban, P., Mach, F., Kůs, P., Pánek, D., Doležel, I., Numerical Solution of Coupled Problems Using Code Agros2D, Computing 95 (2013), No. 1, pp. 381–408.

[9] Solin, P., Cerveny, J., Dolezel, I., Arbitrary-Level Hanging Nodes and Automatic Adaptivity in the hp-FEM, Math. Comput. Simul. 77 (2008), pp. 117–132.

[10] Solin, P. & al, Hermes, URL: http://www.hpfem.org/hermes.

(Received: 29. 09. 2015, revised: 1. 12. 2015)